

Transmissibility of coronavirus and its variants from infected subjects in indoor environments

S Anand

Bhabha Atomic Research Centre

Jayant Krishan

Bhabha Atomic Research Centre

B Sreekanth

Bhabha Atomic Research Centre

Y S Mayya (✉ ysmayya@iitb.ac.in)

Indian Institute of Technology Bombay

Article

Keywords: aerosol, COVID-19, coronavirus, risk

Posted Date: May 12th, 2022

DOI: <https://doi.org/10.21203/rs.3.rs-1612071/v1>

License: © ⓘ This work is licensed under a Creative Commons Attribution 4.0 International License. [Read Full License](#)

Version of Record: A version of this preprint was published at Scientific Reports on August 19th, 2022. See the published version at <https://doi.org/10.1038/s41598-022-17693-z>.

Abstract

A central issue in understanding the relative rapidity of transmission of different coronavirus variants pertains to linking the viral load in infected subjects to the lung deposition probability in exposed individuals through detailed aerosol dynamics modelling. In this paper, we specifically focus on indoor scenarios and formulate a double Poisson model to estimate the probability that at least one carrier particle containing at least one virion will be deposited in the lungs and infect a susceptible individual. Unlike the hitherto used single Poisson models, the double Poisson model accounts for fluctuations in the number of carrier particles (droplets or their residues) deposited in the lung in addition to the fluctuations in the number of virions per carrier particle. Using the above formulation, the infection risk is evaluated as a function of viral load using a comprehensive droplet evaporation-settling-dispersion model, weighted droplet emissions for expiratory events, and consideration of protection barriers. The model demonstrates that if the viral load changes from 2×10^8 RNA copies/mL to 2×10^{10} RNA copies/mL for a 10-minute exposure period in a typical indoor environment, the risk increases rapidly from 1–50%. As the viral load exceeds 10^9 RNA copies/mL, the model predicts a smooth shift from log-log linear behaviour to that of a saturating function approaching unity. These estimates explain the greater transmissibility observed in the case of Delta and Omicron variants, which produce a higher viral load than older wild SARS-CoV-2 variants. The implications are further discussed.

Introduction

More than 8.2 billion vaccine doses have been administered across 182 countries worldwide to prevent the COVID-19 disease, and ~48% of the global population is fully vaccinated against SARS-CoV-2 virus (<https://covid19.who.int>). The overall pattern of the coronavirus pandemic so far has been a series of COVID-19 waves in several parts of the globe. The outbreak peaks were each caused by early strains of SARS-CoV-2, the Beta variant, or the Delta variant. The recent increase in the number of infections at a faster rate is due to the new variant, Omicron^{1,2}. Thus, the emergence of pandemic has seen an increasingly transmissibility associated with each variant/phase of the disease. The rate of propagation/transmissibility is defined through a measure, which is a reciprocal of time to reach a given risk. Since new mutant variants of SARS-CoV-2 virus have different infectious characteristics, it is very important to study the factors that control indoor infection risk using comprehensive model^{1,3-5}. This will help in understanding the disease spread and infection risk related to low and medium risk events apart from superspreading scenarios.

Despite an initial epistemic uncertainty, the aerosol route is now recognized as the principal path of transmission of COVID-19. A comprehensive risk model through aerosol route was proposed by Nicas et al. in 2005⁶ for the airborne infectious diseases. Similar to this model, several infection risk estimation models are developed in the recent times to quantify the risk posed by the COVID-19 infected subjects in the indoor environments^{2,7-12}. These single hit models are based on the deposition of a single virus as the initiating factor of the disease which relegates the viral content of the droplets to the secondary factors such as droplet size, virion concentration in saliva or mucus. The important deviation in these models is, inhaled droplet volume is treated as continuous and Poisson fluctuations are assigned to the occurrence events of virus in the total inhaled droplet volume. However, this lacks generality, just as the virions are discrete, the droplet inhalation is also a discrete process. In order to get one virion deposited in the lung, one must inhale at least one droplet. This calls for a double Poisson probability approach which has been incorporated successfully in the present model.

Another important aspect of the risk model is coupling of droplet evaporation process with other dynamical processes such as dispersion in the indoor space and gravitational settling. The precise modelling of evaporation of droplets containing non-volatile salts is a complex process, and hence many risk models assume a constant final diameter of the droplets (ex. ~50% of their initial value at the emission). The present seamless coupled modelling approach eliminates the dichotomous approach of assigning the settling velocities either only to dry/wet particles. In this model, the dispersion mechanism is treated by the ventilation dependent turbulent diffusion process in which the diffusion coefficient is phenomenologically related to the air-exchange rate. The deposition of the airborne virus-laden droplets in the human respiratory tract is another important process demands an attention since it is a strong function of droplet size and dimension of the parts of respiratory system. Also, there are growing evidence that different variants infect different parts of respiratory system, for example, recent studies show that Omicron variant infects and multiplies faster than the original and Delta variants in human bronchus¹³. In the present work, both bronchial and pulmonary deposition events are taken into consideration through empirical relation based on standard ICRP lung deposition model¹⁴.

A comparison of risk estimation models from the literature along with the present model is given in the Table 1. Most of them are based on quanta generation rate and Wells-Riley “one-hit” risk hypothesis (single Poisson model for infection risk), and concerned more about superspreading events. Although qualitatively, there is an understanding about the impact of viral load on the infection risk, the following question remains unanswered – how enhanced viral load (infectivity of the disease) increases the transmissibility of the disease, mediated by aerosol route? The missing link can only be addressed by coupling the viral load to the aerosol mechanics.

The present study focuses on the indoor problem as a more essential aspect in the disease's spread at this stage, in light of the controlled functioning of socioeconomic activities around the world. While doing so, we incorporate large number of factors which control this propagation such as wearing of mask, observing appropriate COVID-19 behaviour, indoor air cleaner and air cleaning mechanisms, effect of ambient parameters such as temperature, relative humidity, etc. To take effective measures, a fundamental question to be understood is how exactly the aerosol route contributes to transmission; and equally important, how does it depend on the virulence of the viral variants. These questions can be answered by estimating the risks of inhalation of a susceptible person subject to potential exposure through a quantitative modelling of aerosol behavior. The connection between the viral load and the degree of transmissibility (propagation rate) is established by considering the time of interaction required to attain a given level of risk between a susceptible and infected person, modes of infection that include acute cases of coughing and sneezing with moderate breathing and speech. The results are discussed in the following sections.

Results And Discussion

Model

The present model recognizes not only the discreteness of virions and its fluctuations but also that of the inhaled residues/droplets which vector them and hence, introduces fluctuations in the entire size spectrum¹⁷⁻¹⁹. Thus, the probability of at least one virus being deposited in a lung is proportional to the likelihood of inhaling at least one droplet containing at least one virion. A double Poisson distribution function is used to represent these probabilities, which is illustrated here:

Table 1
Comparison of infection risk models

	Nicas et al. ⁶	Buonano et al. ⁷	Buonano et al. ¹⁵	Dhawan et al. ¹¹	Peng et al. ⁹	Mizukoshi et al. ⁸	Azuma et al. ¹⁶	Sussman et al. ¹²	Netz et al. ¹⁰
Emission	Coughing, sneezing	Breathing at different conditions	Speaking, breathing, counting	Sneezing, coughing, speaking	Speaking, breathing, singing, exercise	Coughing, speaking	Coughing, speaking	Breathing, Speaking, Coughing	Speaking
Size distribution	Discrete	Discrete	Total volume	Continuous	Total volume	Discrete	Discrete	Total volume	Continuous
Virusol	Same viral load as the sputum								
Evaporation of droplets	Parameterization, 50% reduction assumed	Not considered	Dehydrated volume is considered	Calculated for each size	Not considered	Not considered	Not considered	Started with evaporated droplet nuclei	Calculated for each size
Ventilation effect	Uniformly mixed, first-order rate	Uniformly mixed, first-order rate	Uniformly mixed, first-order rate	Diffusion, gravitational settling, and ambient air flow	Uniformly mixed, first-order rate	Uniformly mixed, first-order rate	Uniformly mixed	Uniformly mixed	Settling under gravity with evaporation
Gravitational settling	Stirred settling formula	Constant, 0.24 h ⁻¹	Constant, 0.24 h ⁻¹		Neglected	First-order rate	-	-	
Airborne inactivation	Yes, first-order rate	Constant, 0.63 h ⁻¹	Constant, 0.63 h ⁻¹	Considered	Neglected	Considered	Yes + sterilization	Considered	Neglected
Air-cleaning factor	Yes, first-order rate	No	No	No	Yes, first-order rate	No	No	No	-
Respiratory deposition	Yes	No	No	Yes, ICRP model	No	No	No	No	No
Risk model	Single-hit & multiple-hit	Single-hit	Single-hit	Single-hit	Single-hit	Single-hit	Single-hit	Single-hit,	No
Infectivity factor	No	Yes	Yes, PFU	Yes	Quanta emission	Yes, PFU	Quanta emission	Infective quanta	No
Variation of input parameters	Constant	Constant	Prob. density function	Yes, for some parameters	Yes	Yes	Yes	Yes	Yes
Protection factor	No	No	No	Mask & distance	Mask	Mask	No	Discussed qualitatively	No
Re-suspension	No	No	No	No	No	No	Introduced	No	No

Suppose a person inhales a typical number of droplets (N_d), each of which is expected to contain an average number of virions, n_v . The risk of breathing at least one virion is then given by $R = 1 - \exp(-N_d n_v)$ according to the single Poisson fluctuation model, which implies that there are fluctuations in the number of virions in the droplet but not in the number of droplets inhaled. The number of droplets inhaled would, however, fluctuate around the mean value at low droplet concentrations. As a result, the risk formula is modified to factor for both fluctuations, and the modified risk for inhalation of at least one droplet carrying a virion can be expressed as,

$$R' = 1 - \exp(-N_d [1 - \exp(-n_v)])$$

1

The main difference is that in the modified formula (Eq. (1)), the values N_d and n_v appear separately, rather than as a product, which is commonly employed in the literature^{6-11,15}. In the present study, the above formula has been combined with averaging over the polydisperse size distribution function. The present double Poisson model has the advantage of being applicable even in the case of extremely low risk scenarios, such as inhalation for a brief period or at low droplet number concentrations.

To demonstrate the applicability of this model, a standard inhalation infection risk problem⁶ is used, in which four discrete droplet diameters (4.2 μm (1200 droplets), 9.0 μm (100 droplets), 14.6 μm (6.2 droplets) and 18.8 μm (1.7 droplets)) are released during coughing event (10 h^{-1}) in room volume of 50 m^3 with an air-exchange rate of 0.5 h^{-1} . In this scenario, a viral load of ($5 \times 10^6 - 5 \times 10^{10}$) \#/mL in the biological fluid is considered, with 0.1 h^{-1} inactivation rate. The risk estimates from the current model (Eq. (1)) are compared to those of Nicas et al.⁶ using these input values, as shown in Table 2. In the comparison table, the implications of separating the fluctuations in inhaled droplets from the likelihood that a droplet is infected are shown.

Table 2
Comparison of risk with Nicas et al.⁶

Initial droplet diameter, μm	Single-hit risk					
	$C_v = 5 \times 10^6 \text{ mL}^{-1}$		$C_v = 5 \times 10^8 \text{ mL}^{-1}$		$C_v = 5 \times 10^{10} \text{ mL}^{-1}$	
	Present model	Nicas et al. ⁶	Present model	Nicas et al. ⁶	Present model	Nicas et al. ⁶
4.2	4.89E-04	1.93E-03	4.73E-02	1.76E-01	8.97E-01	1.00E+00
9.0	5.21E-03	5.89E-03	3.81E-01	4.46E-01	9.47E-01	1.00E+00
14.6	1.03E-03	9.07E-05	6.99E-02	9.03E-03	1.27E-01	5.96E-01
18.8	4.00E-04	4.62E-06	1.96E-02	4.62E-04	2.42E-02	4.52E-02

When compared to Nicas et al.⁶, the projected risk from the current model for the 4.2 μm droplet is four times lower for $C_v \leq 5 \times 10^8 \text{ mL}^{-1}$ (Table 2), owing to the difference in final droplet size, which determines its lifetime and lung deposition characteristics. In the case of larger size droplets (14.6 μm and 18.8 μm), the risk estimates from these two models differ by a ratio of $\sim(8$ to 90). According to the current simulation results, the final droplet diameter is decreased to $\sim 1/5$ th of the original droplet (Fig. 1) as opposed to 50% reduction in Nicas et al.⁶ due to evaporation. The difference in the equilibrium droplet size is mainly due to the solid content in the saliva/droplet apart from other ambient conditions. In the present work, a solid content of 8 g/L is assumed as against 88 g/L in Nicas et al.⁶, and the evaporation of droplet is modelled precisely and coupled with the other processes seamlessly. Also, Nicas et al.⁶ assumes that the droplets released are instantaneously mixed in the room environment and hence the concentration is uniform whereas, the present studies include the effect of ventilation induced turbulence to simulate the dynamics of the droplets in the room.

A recent study by Lieber et al.²⁰ also shown that a mass concentration of salts and proteins of 0.8% in the saliva droplets will result in a ratio between equilibrium and initial diameter of 20%. This difference in the final droplet size leads to different sedimentation velocity that modifies the residence time of droplets in the indoor environment, and lung deposition fraction to estimate the inhalation risk. Also, the fluctuation in the low droplet number concentration (for 14.6 μm and 18.8 μm sizes) contribute to the variation in the risk estimation. In the case of higher viral load, the risk estimates from these two models are closer since $1 - exp(-\mu)$ tends to 1 due to high viral load, and other effects compensate each other. Although final risk estimates from these two models are nearly same in some cases, large difference is observed in handling individual processes. Hence, it is recommended to couple the physical processes as much as possible and run the dynamic model to arrive at realistic estimates. In the present study, falling-to-mixing-plate-out model²¹ is implemented, which allows a droplet's residence time (τ) to smoothly transition from a gravity-dominated (larger particles, diameter $> 50 \mu\text{m}$, $\tau < 100 \text{ s}$) to a turbulence-dominated (small particle, diameter $< 5 \mu\text{m}$, $\tau > 3000 \text{ s}$) regime as shown in Fig. 1. It's worth mentioning that turbulent mixing extends the particle residence time for droplets of intermediate size. The variation of droplet lifetime with RH is significant only for large particles of diameter in the range of 20–80 μm , mainly due to the effect of evaporation and gravitational settling in this size regime. The lifetime of virusols in the indoor environment is mostly determined by deposition; however, viral deposition in the lungs is completely determined by viral load and aerosol physics. The current study provides a common factor for risk estimation, bringing universality to the modified risk formula.

Single-hit risk and reproduction number

Present study attempts to calculate the exposure time required to achieve a tangible single-risk for a given expiratory event as well as the reproduction number (R_0) for the given input parameters. Coughing and sneezing will be specific to the sick and symptomatic patients, although breathing and speaking are normal expiratory processes relevant to all subjects. Table 3 lists the parameters of expiratory emission, such as droplet size distribution, frequency of emission, virion concentration in emitted droplets, etc.

Table 3
Emission characteristics of expiratory events

Expiratory events	Size distribution parameters	Number release rate*	References
Breathing	CMD = 1.6 μm ; GSD = 1.3	14 s^{-1} (continuous)	Johnson et al. ³²
Coughing	CMD = 14 μm ; GSD = 2.6	28 s^{-1} (10 cough/h)	Duguid ¹⁷
Speaking	CMD = 4 μm ; GSD = 1.6	270 s^{-1} (5 min/h)	Johnson et al. ³² ; Alsvet et al. ³³
Sneezing	GM = 8.1 μm ; GSD = 2.3	2778 s^{-1} (10 sneezes/h)	Duguid ¹⁷

* - long-time averaged droplet release rate

For each expiratory event, numerical computations are used to determine the exposure time for different risk levels (0.1%, 1%, 10%, and 50%) and AERs ($0.5 \text{ h}^{-1} - 10 \text{ h}^{-1}$). In the exposure time calculations, it is assumed that the emissions are continuous with the given rate and the value is estimated for a given risk. The model findings (Fig. 2) reveal that, up to a critical viral load, the exposure duration decreases linearly with the viral load in the log-log graph. Although the findings are not shown here, the slope of the linear component increases with emission rate (S_0). The critical viral load in this case is, 10^{13} \#/mL for breathing, 10^{11} \#/mL for coughing, 10^{10} \#/mL for sneezing, 10^{12} \#/mL for speaking for a risk of 0.1%. Beyond the critical viral load, the risk becomes a constant or invariant w.r.to viral load.

Alternative to the exposure time estimates, single-hit risk is estimated under the influence of all the four expiratory events occurring simultaneously at given emission rates. The joint risk probability is then given by,

$$R' = 1 - P_{0,B} \times P_{0,Sp} \times P_{0,C} \times P_{0,Sn}$$

2

where $P_{0,B} = \exp(-N_d [1 - \exp(-n_v)])$ is the probability of zero-hit for breathing expiratory process, the suffices Sp , C and Sn denotes speaking, coughing and sneezing events respectively. It is to be noted that transmissibility of a virus is measured via single-hit risk probability, dominated by the aerosol route of exposure. Also, it has been argued often that the transmissibility of the virus is linked with the viral load^{22,23}, and hence, the risk of transmission to a susceptible individual is estimated as a function of viral load for specified exposure times (Fig. 3).

Numerical results (Fig. 3a) shows that the risk is less than 1% for viral loads $< 10^8$ RNA copies/mL for 1-hour exposure period. But the risk rapidly approaches higher value (ex. 50% for 10^{10} RNA copies/mL and 10-min exposure), which demonstrates the high transmissibility of Delta and possibly Omicron variants which are reported to give rise to higher viral loads²⁴⁻²⁸ (Table 4). The disease's actual severity, on the other hand, is linked to its biological infectivity. Thus, the present study clearly demonstrates the dependence of risk on the viral load irrespective of variants. The model also explores the effect of ventilation rate on indoor infection risks (Fig. 3b). When the air-exchange rate is increased from 0.5 h^{-1} to 10 h^{-1} for a 10-minute exposure time, the single-hit risk decreases approximately by an order. This is primarily due to the elimination of airborne viruses from the indoor environment via ventilation. However, when viral load increases, the effect of enhancing ventilation reduces because smaller particles contribute to the risk as well. The ambient RH has only a minor impact on the risk; higher RH leads to larger final droplet sizes, which reduces their lifetime and therefore infection risk, as seen in Fig. 3b.

Figure 3a: Variation of single hit risk for susceptible persons as a function of viral load for different time of exposure

Table 4
Typical viral load of SARS-CoV-2 variants²⁴⁻²⁸

SARS-CoV-2 variant	Viral load (RNA copies/mL)
Wild	$\sim 10^5 - 10^8$
Delta	$\sim 10^6-10^9$
Omicron	$\sim 10^6-10^{9.5}$

Another essential metric to describe infection risk is the reproduction number (R_0), which is computed by multiplying the infection risk during the exposure time of each susceptible person by the number of susceptible people exposed for a specific exposure scenario. The following two scenarios are studied in this work to demonstrate how the model can be used: a) 25 students in a classroom with an infected subject exposed for four hours; b) 4 employees in an office environment with an infected subject exposed for eight hours. The R_0 value approaches 2 when the viral load of infected person in the class room exceeds $5 \times 10^7 \text{ \#/mL}$, as shown in the results; also, the R_0 value shall remain ≤ 1 if the viral load is less than $2.5 \times 10^7 \text{ \#/mL}$ for the given input and environmental parameters, as shown in Fig. 4. Similarly, if the viral load is $\leq 7 \times 10^7 \text{ \#/mL}$ for the given exposure conditions in an office setting, the R_0 value will be ≤ 1 . These findings imply that if the viral load is less than a certain value or if the contact period is limited for the specified emission and indoor settings, the reproduction number will remain less than one. Alternatively, the limit on number of people can also be estimated using the present approach for a given virus variant and the exposure duration. Hence, these studies can be used as a tool to aid decision/policy making as the spread of the disease can be directly predicted based on the viral load and other physically measurable input parameters.

Conclusion

In this study, we investigate the crucial relationship between viral load and the transmissibility of respiratory viruses in the indoor environment. This is accomplished by considering the aerosol dynamics of evaporating droplets as well as fluctuations in the virion deposition probability in the lungs (both virions and droplets). The model accounts for several factors that influence infection risk, such as infected subject's mode of emission, droplet characteristics, indoor environment parameters (air humidity, ventilation, and turbulence), and protection factors (mask, air cleaners). The model can seamlessly handle cases of ultra-low risk ($< 1\%$), as well as those approaching unity, because it handles fluctuations both in the virion content in a droplet and deposition probability in the lung through a double Poissonian model. At a formulation level, the present work introduces a paradigm shift through double Poissonian approach as opposed to earlier single Poisson model for estimating the inhalation risk via the aerosol route across a wide range of exposure conditions, i.e. from ultra-low risk to unity. Model results show that as the viral load increases, saturation effect occurs i.e. larger fraction of droplets are virus laden and hence, the entire expiratory ejecta has the potential to contribute to transmission of the disease. For a four-hour exposure in a classroom with 25 students, the reproduction

number is estimated to be less than 1 for viral loads $\leq 3 \times 10^7$ RNA copies/mL and is more than 2 for viral loads $> 10^8$ RNA copies/mL. This critical dependence of risk on the viral load, explains the crucial observations of relatively higher transmission rate of Delta and Omicron variants via the viral load factor. The study puts in to perspective the effectiveness of technologies such as masks, air cleaners, and external ventilation in regulating infection risk. This is an especially attractive feature of the model since it will be useful in determining the cost-effectiveness of technology deployment.

Among various parameters examined, this model shows a dominating effect of the viral load, which is related to the variant type, on the risk of transmitting the disease to a susceptible member in a cohort. We believe that the double Poissonian formalism combined with the comprehensive aerosol dynamics model introduced here makes a significant value addition to the subject of risk evaluation of airborne diseases. Equally importantly, it will help at a policy level for assessing the potential rapidity of the spread of the emerging variants from the information available on viral load in patients.

Materials And Methods

Consider an infected person in an indoor environment who speaks, breathes, coughs, and sneezes, releasing droplets in air. By applying the "Falling-to-Mixing-Plate-out" model²¹ to the modified risk formula (Eq. (1)), the infection risk for inhalation of at least one droplet carrying a virion (single-hit hypothesis) by a susceptible in the room environment is given by,

$$R' = 1 - P_0 = 1 - e^{-kC_0 \left\{ \int_{d_p^{min}}^{d_p^{max}} f_r(d_p) F_L(d_p) (1 - e^{-\mu}) dd_p \right\}}$$

3

where P_0 is the probability of zero-hit, $k = \frac{1}{V_{room} \lambda_{eff}} PF_1 PF_2 q_B t_{expos}$ is a constant, $C_0 = S_0 \int_0^\infty f_e(d_w) dd_w$ is total number concentration of original droplets suspended in room, $f_r(d_p)$ is the size distribution of the residues that undergone evaporation in the room, $F_L(d_p)$ is the lung deposition fraction, $\mu = \frac{\pi}{6} \gamma^3 d_p^3 C_v'$, and d_p is the particle diameter, d_p^{min} and d_p^{max} are the minimum and maximum diameter of the evaporated droplet considered for the calculations. In Eq. (3), double Poisson fluctuation theory is introduced to account for statistics on droplet fluctuation as well as the probability of virus incorporation in droplets (virusolization).

PF_1 and PF_2 are the protection factors due to the masks/face shields worn by the infected and healthy person respectively, provide additional measures (deposition of emitted droplets) in reducing the spread of infection from both the emitter and receiver sides. q_B is the breathing rate of the healthy person, t_{expos} is the exposure time, and V_{room} is the room volume. S_0 is the total droplet emission rate, $f_e(d_w)$ is the exhaled droplet number-size distribution, and d_w is the wet droplet diameter. γ is the ratio of wet droplet diameter (d_w) to evaporated droplet (residue) diameter (d_p). The droplet residue size is determined by the droplet composition and their mass. It is noted to be here that the all dynamics of settling is controlled by the size of the residue but the airborne virion concentration is prescribed by the wet droplet size.

$C_v' = C_v \frac{\lambda_{eff}}{\lambda_d + \lambda_{eff}}$ is the virion concentration corrected for its decay (inactivation), λ_d is the inactivation rate of pathogens, and C_v is the viral load in the biological fluid. The natural decay of virion causes differential dilution of viral load in droplets, and plays an important role in limiting the residence time in certain cases and its inclusion in the model is essential. λ_{eff} is the effective removal rate due to ventilation²⁹, gravitational settling, bulk diffusion³⁰ and wall deposition. The model takes into account the effect of ventilation caused by one or more of the following elements: fan, air cleaner, and natural air exchange. The deposition of residues in the respiratory system of susceptible person is obtained by multiplying the residue number concentration distribution from the indoor model by the lung deposition probability function in the bronchial and pulmonary region given by,

$$F_L(d_p) = \left(0.0315 d_p^{-0.9} + 0.48 d_p^{1.85} \right) e^{-1.29 d_p^{0.76}}$$

4

where d_p is the particle diameter in micron. Eq. (4) is constructed by fitting the deposition fraction curve from ICRP 66¹⁴ between 0.1 μm to 30 μm (Fig. 5).

Eq. (3) calculates the infection risk, which is a measure of the disease's reproduction number and transmissibility for a given viral load apart from the person's disease state and variant type (old wild, Delta or Omicron). This modified risk model is implemented in Mathematica³¹ and the findings are presented in the Results and Discussion sections for various exposure scenarios.

List Of Symbols

C_0 - Viral load in the biological fluid, RNA copies/mL
 τ - Droplet residence time, s
 RH - Relative humidity (50-90%)
 AER - Air exchange rate, h⁻¹
 S_0 - Total droplet emission rate, #/s
 R_0 - Reproduction number
 R - Infection risk for inhalation of at least one droplet carrying a virion (single-hit hypothesis) corresponding to single Poisson probability
 R' - Infection risk for inhalation of at least one droplet carrying a virion (single-hit hypothesis) corresponding to single Poisson probability
 P_0 - Probability of zero-hit
 $P_{0,B}$ - Probability of zero-hit for breathing
 $P_{0,Sp}$ - Probability of zero-hit for speaking
 $P_{0,C}$ - Probability of zero-hit for coughing
 $P_{0,Sn}$ - Probability of zero-hit for sneezing
 d_w - Wet droplet diameter, μm
 d_p - Evaporated droplet (residue) diameter, μm
 d_p^{min} - Minimum evaporated droplet (residue) diameter, μm
 d_p^{max} - Maximum evaporated droplet (residue) diameter, μm
 γ - Ratio of wet droplet diameter (d_w) to evaporated droplet (residue) diameter (d_p)
 C_0 - Total number concentration of original droplets suspended in room, #/m³
 $f_r(d_p)$ - Size distribution of the residues that undergone evaporation in the room
 $F_L(d_p)$ - Lung deposition fraction in the bronchial and pulmonary region
 C'_0 - Virion concentration corrected for its decay (inactivation), #/m³
 λ_d - Inactivation rate of pathogens (0.63 h⁻¹)²⁴
 λ_{eff} - Effective virus removal rate due to ventilation, h⁻¹
 N_d - Typical number of droplets inhaled by a person
 n_v - Average number of virions in a droplet
 PF_1 - Protection factor due to the masks/face shields worn by the infected person (0.1)
 PF_2 - Protection factor due to the masks/face shields worn by the healthy person (0.1)
 \dot{q}_B - Breathing rate of the healthy person (10 lpm)
 t_{expos} - Exposure time
 V_{room} - Room volume (100 m³)
 $f_d(d_w)$ - Exhaled droplet number-size distribution
 T_{amb} - Ambient temperature (25°C)
 T_d - Droplet temperature (35°C)
 CMD - Count median diameter
 GSD - Geometric standard deviation
 Z_1 - Room height (4 m)
 H - Release height (1.5 m)

Declarations

Author Contributions:

Y.S.M. and S.A. designed research; J.K. and B.S. performed numerical simulations; S.A., J.K., B.S. and Y.S.M. analyzed data; and S.A., J.K., B.S. and Y.S.M. wrote the paper.

Competing Interest Statement: The authors declare no competing interest.

Data Availability Statement: All data generated or analysed during this study are included in this published article.

References

- Chen, J.; Wang, R.; Gilby, N. B.; Wei, G.-W. Omicron Variant (B.1.1.529): Infectivity, Vaccine Breakthrough, and Antibody Resistance. *J. Chem. Inf. Model* 2022, 62, 412–422.
- Rodriguez-Rivas, J.; Croce, G.; Muscat, M.; Weigt, M. Epistatic models predict mutable sites in SARS-CoV-2 proteins and epitopes. *Proc. Natl. Acad. Sci. U. S. A.* 2022, 119(4), e2113118119.
- Coldrick, S.; Kelsey, A.; Ivings, M.J.; Foat, T.G.; Parker, S.T.; Noakes, C.J.; Bennett, A.; Rickard, H.; Moore, G. S. Modeling and experimental study of dispersion and deposition of respiratory emissions with implications for disease transmission. *Indoor Air* 2022, 32(2), e13000.
- Wood, R. M.; Egan, J. R.; Hall, I. M. A dose and time response Markov model for the in-host dynamics of infection with intracellular bacteria following inhalation: with application to *Francisella tularensis*. *J. R. Soc. Interface* 2014, 11, 20140119.
- Bathula, S.; Anand, S.; Thajudeen, T.; Mayya, Y.S.; Chaudhury, P.; Shashank, C. Survival of expiratory aerosols in a room: Study using a bi-compartment and bi-component indoor air model. *Aerosol Air Qual. Res.* 2021, 21, 200547.
- Nicas, M.; Nazaroff, W. W.; Hubbard, A. Toward understanding the risk of secondary airborne infection: Emission of respirable pathogens. *J. Occup. Environ. Hyg.* 2005, 2, 143–154.
- Buonanno, G.; Stabile, L.; Morawska, L. Estimation of airborne viral emission: Quanta emission rate of SARS-CoV-2 for infection risk assessment. *Environ. Int.* 2020, 141, 105794.

8. Mizukoshi, A.; Nakama, C.; Okumura, J.; Azuma, K. Assessing the risk of COVID-19 from multiple pathways of exposure to SARS-CoV-2: Modeling in health-care settings and effectiveness of nonpharmaceutical interventions. *Environ. Int.* 2021, 147, 106338.
9. Peng, Z.; Pineda Rojas, A.L.; Kropff, E.; Bahnfleth, W.; Buonanno, G.; Dancer, S.J.; Kurnitski, J.; Li, Y.; Loomans, M.G.L.C.; Marr, L.C.; Morawska, L.; Nazaroff, W.; Noakes, C.; Querol, X.; Sekhar, C.; Tellier, R.; Greenhalgh, T.; Bourouiba, L.; Boerstra, A.; Tang, J.W. *et al.* Practical Indicators for Risk of Airborne Transmission in Shared Indoor Environments and Their Application to COVID-19 Outbreaks. *Environ. Sci. Technol.* 2022, 56, 1125–1137.
10. Netz, R. R. Mechanisms of Airborne Infection via Evaporating and Sedimenting Droplets Produced by Speaking. *J. Phys. Chem. B* 2020, 124, 7093–7101.
11. Dhawan, S.; Biswas, P. Aerosol Dynamics Model for Estimating the Risk from Short-Range Airborne Transmission and Inhalation of Expiratory Droplets of SARS-CoV-2. *Environ. Sci. Technol.* 2021, 55, 8987–8999.
12. Sussman, R. A.; Golberstein, E.; Polosa, R. Aerial Transmission of the SARS-CoV-2 Virus through Environmental E-Cigarette Aerosols: Implications for Public Policies. *Int. J. Environ. Res. Public Health* 2021, 18(4):1437.
13. Hui, K. P. Y.; Ho, J. C. W.; Cheung, M.; Ng, K.; Ching, R. H. H.; Lai, K.; Kam, T.T.; Gu, H.; Sit, K.Y.; Hsin, M. K. Y.; Au, T. W. K.; Poon, L. L. M.; Peiris, M.; Nicholls, J. M.; Chan, M. C. W. SARS-CoV-2 Omicron variant replication in human bronchus and lung ex vivo. *Nature* 2022, 603, 715-720.
14. International Commission on Radiological Protection, Human respiratory tract model for radiation protection. *Oxford Pergamon Press*, ICRP Publication 66 (1994).
15. Buonanno, G.; Morawska, L.; Stabile, L. Quantitative assessment of the risk of airborne transmission of SARS-CoV-2 infection: prospective and retrospective applications. *Environ. Int.* 2020, 145, 106112.
16. Azuma, K.; Yanagi, U.; Kagi, N.; Kim, H.; Ogata, M.; Hayashi, M. Environmental factors involved in SARS-CoV-2 transmission: effect and role of indoor environmental quality in the strategy for COVID-19 infection control. *Environ. Health Prev. Med.* 2020, 25, 66.
17. Duguid, J. P. The size and the duration of air-carriage of respiratory droplets and droplet-nuclei. *J. Hyg. (Lond)*. 1946, 44, 471–479.
18. Anand, S.; Mayya, Y. S. Size distribution of virus laden droplets from expiratory ejecta of infected subjects. *Sci. Rep.* 2020, 10, 21174.
19. Stadnytskyi, V.; Bax, C. E.; Bax, A.; Anfinrud, P. The airborne lifetime of small speech droplets and their potential importance in SARS-CoV-2 transmission. *Proc. Natl. Acad. Sci.* 2020, 117 (22), 11875-11877.
20. Lieber, C.; Melekidis, S.; Koch, R.; Bauer, H.-J. Insights into the evaporation characteristics of saliva droplets and aerosols: Levitation experiments and numerical modeling. *J. Aerosol Sci.* 2021, 154, 105760.
21. Anand, S.; Krishan, J.; Bathula, S.; Mayya, Y. S. Modeling the viral load dependence of residence times of virus-laden droplets from COVID-19-infected subjects in indoor environments. *Indoor Air* 2021, 31, 1786–1797.
22. Riediker, M.; Briceno-Ayala, L.; Ichihara, G.; Albani, D.; Poffet, D.; Tsai, D.H.; Iff, S.; Monn, C. Higher viral load and infectivity increase risk of aerosol transmission for Delta and Omicron variants of SARS-CoV-2. *Swiss Med. Wkly.* 2022, 152, w30133.
23. Li, B.; Deng, A.; Li, K.; Hu, Y.; Li, Z.; Shi, Y.; Xiong, Q.; Liu, Z.; Guo, Q.; Zou, L.; Zhang, H.; Zhang, M.; Ouyang, F.; Su, J.; Su, W.; Xu, J.; Lin, H.; Sun, J.; Peng, J.; Jiang, H. *et al.* Viral Infection and Transmission in a Large, Well-Traced Outbreak Caused by the SARS-CoV-2 Delta Variant. *Nat. Commun.* 2022, 13(1), 460.
24. Mikszewski, A.; Stabile, L.; Buonanno, G.; Morawska, L. Increased close proximity airborne transmission of the SARS-CoV-2 Delta variant. *Sci. Total Environ.* 2022, 816, 151499.
25. von Wintersdorff, C. J. H.; Dingemans, J.; van Alphen, L.; Wolffs, P.; van der Veer, B.; Hoebe, C.; Savelkoul, P. Infections caused by the Delta variant (B.1.617.2) of SARS-CoV-2 are associated with increased viral loads compared to infections with the Alpha variant (B.1.1.7) or non-Variants of Concern. *PREPRINT (Version 1) available at Research Square* 2021.
26. Sender, R.; Bar-On, Y. M.; Gleizer, S.; Bernshtein, B.; Flamholz, A.; Phillips, R.; Milo, R. The total number and mass of SARS-CoV-2 virions. *Proc. Natl. Acad. Sci.* 2021, 118, e2024815118.
27. Teysou, E.; Delagrèverie, H.; Visseaux, B.; Lambert-Niclot, S.; Brichler, S.; Ferre, V.; Marot, S.; Jary, A.; Todesco, E.; Schnuriger, A.; Ghidaoui, E.; Abdi, B.; Akhavan, S.; Houhou-Fidouh, N.; Charpentier, C.; Morand-Joubert, L.; Boutolleau, D.; Descamps, D.; Calvez, V.; Marcelin, A. G.; Soulie, C. The Delta SARS-CoV-2 Variant Has a Higher Viral Load than the Beta and the Historical Variants in Nasopharyngeal Samples from Newly Diagnosed COVID-19 Patients. *J. Infect.* 2021, 83(4), e1–e3.
28. Miguères, M.; Dimeglio, C.; Trémeaux, P.; Raymond, S.; Lhomme, S.; Da Silva, I.; Oliveira Mendes, K.; Abravanel, F.; Félicé, M.-P.; Mansuy, J.-M.; Izopet, J. Influence of the Delta Variant and Vaccination on the SARS-CoV-2 Viral Load. *Viruses* 2022, 14 (2), 323.
29. Foat, T.; Drodge, J.; Nally, J.; Parker, S. A relationship for the diffusion coefficient in eddy diffusion based indoor dispersion modelling. *Build. Environ.* 2020, 169, 106591.
30. Shimada, M.; Okuyama, K.; Okazaki, S.; Asai, T.; Matsukura, M.; Ishizu, Y. Numerical Simulation and Experiment on the Transport of Fine Particles in a Ventilated Room. *Aerosol Sci. Technol.* 1996, 25(3), 242-255.
31. Mathematica, Version 5.2. Wolfram Research, Inc., Champaign, Illinois (2005).
32. Johnson, G. R.; Morawska, L.; Ristovski, Z. D.; Hargreaves, M.; Mengersen, K.; Chao, C. Y. H.; Wan, M. P.; Li, Y.; Xie, X.; Katoshevski, D.; Corbett, S. Modality of Human Expired Aerosol Size Distributions. *J. Aerosol Sci.* 2011, 42(12), 839–851.
33. Alsved, M.; Matamis, A.; Bohlin, R.; Richter, M.; Bengtsson, P.-E.; Fraenkel, C.-J.; Medstrand, P.; Löndahl, J. Exhaled Respiratory Particles during Singing and Talking. *Aerosol Sci. Technol.* 2020, 54(11), 1245–1248.
34. van Doremalen, N.; Bushmaker, T.; Morris, D. H.; Holbrook, M. G.; Gamble, A.; Williamson, B. N.; Tamin, A.; Harcourt, J. L.; Thornburg, N. J.; Gerber, S. I.; Lloyd-Smith, J. O.; de Wit, E.; Munster, V. J. Aerosol and Surface Stability of SARS-CoV-2 as Compared with SARS-CoV-1. *N. Engl. J. Med.* 2020, 382(16), 1564–1567.

Figures

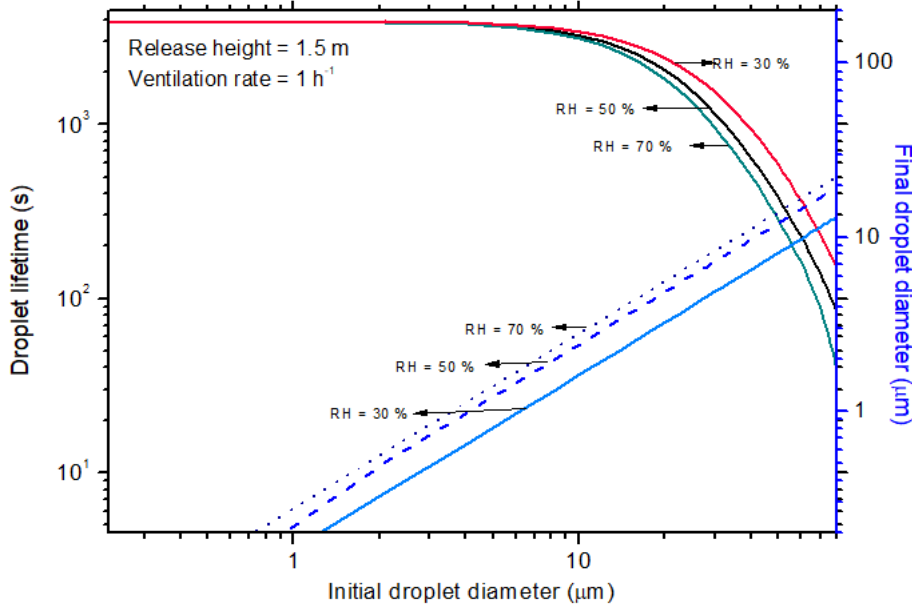


Figure 1

Lifetime of droplets in a typical indoor environment

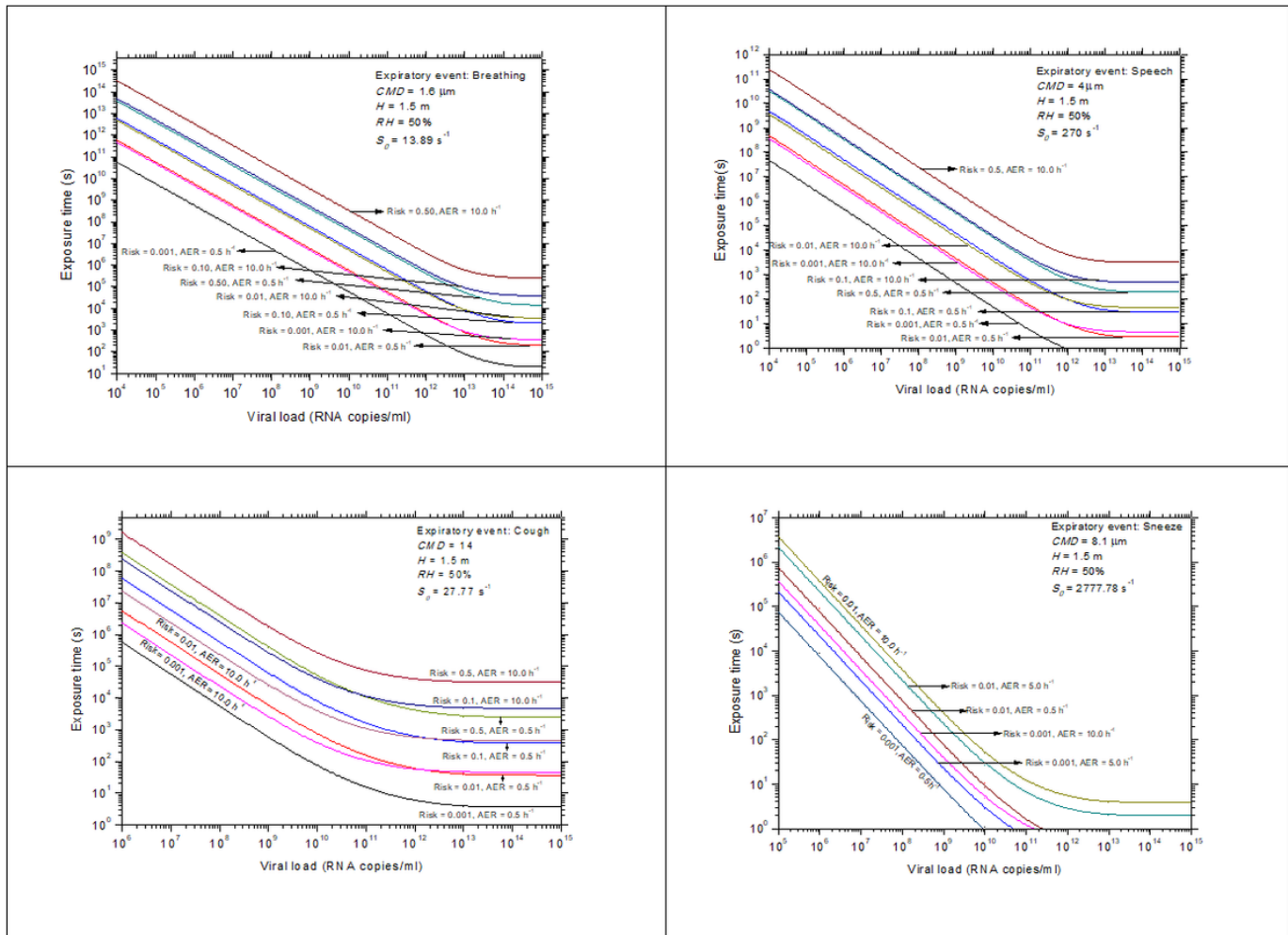
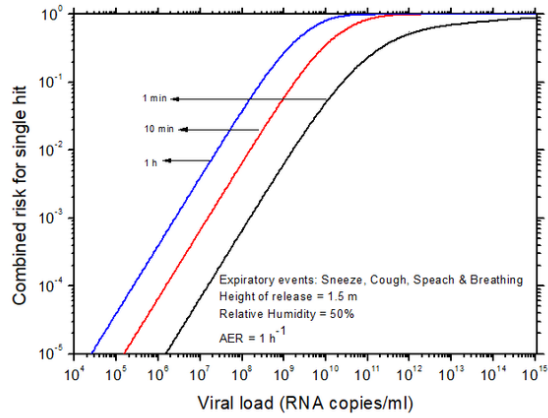
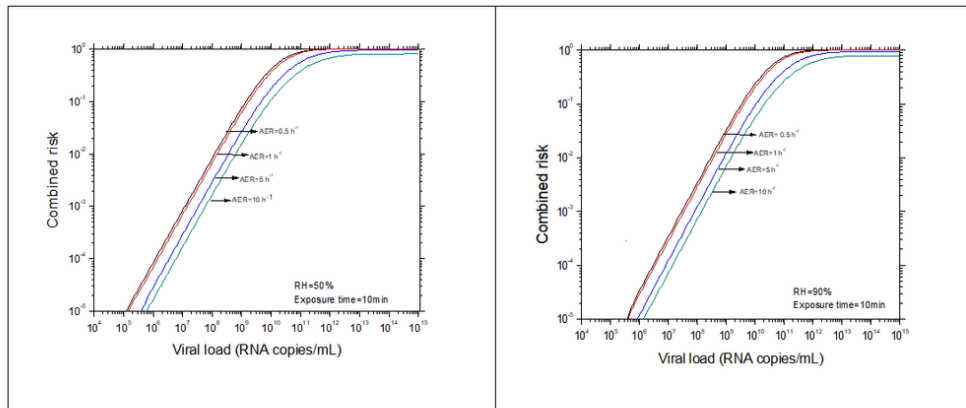


Figure 2

Exposure time as a function of viral load for a given infection risk and ventilation rate in the indoor environment



A



B

Figure 3

a: Variation of single hit risk for susceptible persons as a function of viral load for different time of exposure

b: Variation of single hit risk for susceptible persons as a function of viral load for RH and AER

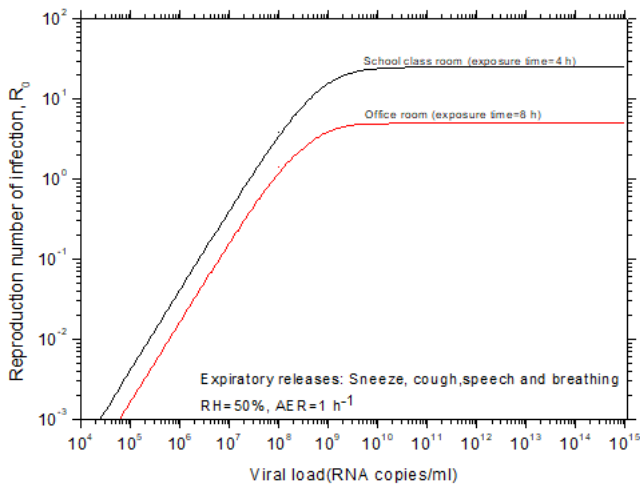


Figure 4

Reproduction number as a function of viral load for two different indoor environments and exposure conditions